

# Impedance spectroscopy characterization of some clay materials

**Mohamed Essaleh<sup>1</sup>, Rachid Bouferra<sup>1</sup>, Mohammed Mansori<sup>2</sup>, Mohamed Oubani<sup>2</sup>, Abdeltif Bouchehma<sup>3</sup>, Amal Bourezza<sup>1</sup> and Soufiane Belhouideg<sup>3</sup>**

<sup>1</sup>Laboratoire de Géosciences, Géoenvironnement et Génie Civil. Cadi-Ayyad University, Faculty of Sciences and Technology, B.P.549, 40000, Marrakech, Morocco

<sup>2</sup>IMED-Lab, Cadi-Ayyad University, Faculty of Sciences and Technology, B.P.549, 40000, Marrakech, Morocco

<sup>3</sup>Research Laboratory of Physics and Engineers Sciences, Team of Applied Physics and New Technologies, Polydisciplinary Faculty (FP-BM), Sultan Moulay Slimane University, Béni Mellal, Morocco

**Abstract:** Impedance spectroscopy technique is considered in this work to study the electrical properties of three types of clays: Rammed earth, Kaolin and Bentonite. The use of these materials is one of the potential ways to support sustainable development in both urban and rural areas. The analysis of their electrical behaviour is a highly important feature for the renewed interest of their use in the building construction. In this context, electrical impedance spectroscopy method with frequency varying between 20 Hz to 1 MHz is used in order to measure electrical complex impedance in a given temperature domain. It permits to give an electric picture of the electrical behaviour of the material and to estimate the activation and relaxation energies for the dominant electrical conduction mechanisms.

**Keywords:** Clay materials, Rammed earth, Kaolin, Bentonite, Impedance spectroscopy.

## 1 INTRODUCTION

The construction sector has a great potential for energy savings and environmental impact reduction by using local bio-based materials. Due to their high physical, thermal, hygroscopic and acoustic properties, they would allow to build healthy, comfortable and energy-efficient habitats (Chandra (2002), Yongkang Huang (2022)). Rammed earth, Kaolin and Bentonite and other clay materials can be used for that purpose for numerous advantages: Sustainability, Micro climate regulation and Sound insulation. Many studies have been published concerning the mechanical and thermal properties of earth-based materials (Yongkang Huang (2022), Saidi (2018); Medjelekh (2017); Miccoli (2014) and Chihab (2018)). Mechanical strength has been of particular interest as it ensures the structural stability of the building. Because of the availability of this raw materials and their low cost, the current trend is to use them in the reinforcement of the building materials. To our knowledge, there are no published works on electrical conduction in terms of temperature and frequency dependence of the electrical conductivity ( $\sigma$ ) of these materials, especially in the high temperature range ( $T > 300^\circ\text{C}$ ) where  $\sigma$  starts to be important. Hence, the aim of this work is to investigate the electrical characteristics of some clay materials (Rammed earth, Kaolin and Bentonite). Continuing our investigation on the disordered semiconducting materials (Bouchehma (2021), Bouferra (2019), Amhil (2019), Essaleh (2017), Essaleh (2018), and Kirou (2019)), the temperature and frequency dependence of the electrical conductivity is considered in order to identify the most dominant electrical conduction mechanisms in these materials.

## 2 EXPERIMENTAL DETAILS

The unfired rammed earth considered in this work was extracted from the region of Marrakech in Morocco while a high quality of Kaolin and Bentonite samples were collected from different commercial societies. Usually and depending on the geological context and geographical positions, these materials are composed of quartz, calcite, dolomite and clay minerals (Chihab (2018) and El Fgaier (2016)). Samples in form of pellets of 13 mm in diameter and 2 mm in thickness using 0.6 g of rammed earth, Kaolin and Bentonite were prepared by uniaxial pressing of 5 MPa and covered on both sides with silver (Ag) electrodes. The various electrical and dielectric parameters (Complex impedance ( $Z^*$ ), capacitance ( $C$ ), dielectric losses ( $D = \tan \delta$ ), electrical conductivity ( $\sigma$ ), Modulus  $M^*$ , etc.) can be measured using an “HP 4284A” impedance meter operating in the frequency domain ranging from 20 Hz to 1 MHz and under an excitation level of the order of (500 mV). The ceramic is placed into a temperature-controlled programmable cylindrical furnace that allows temperatures ranging from 25 °C to 750 °C. A “HP-34401A” type multimeter is used to measure the voltage variation across a K type thermocouple placed close to the sample, in order to follow the evolution of its temperature. The temperature is programmed using a “Eurotherm 2416” type regulator, with a speed of around 5 °C / min. Finally, the whole (impedance-meter, furnace) is controlled automatically by a computer such as it is presented in Fig. 1.

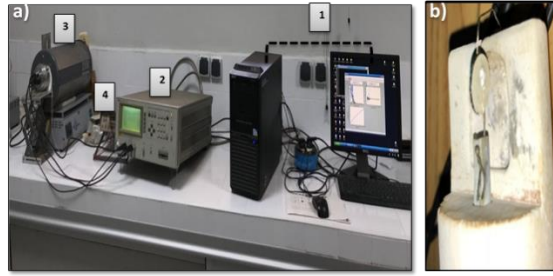


Fig.1: a) Device for measuring the complex impedance at high temperatures. (1): data acquisition system. (2) HP4284A impedance meter. (3) Programmable oven. (4) Temperature display. b) Sample holder cell.

### 3 RESULTS AND DISCUSSION

It is well known that the complex impedance ( $Z^*$ ) and the electric modulus ( $M^*$ ) formalisms are usually used to identify and distinguish the contribution of largest resistance from those of smallest capacitance. According to the classical theory of Debye (Barsoukov (2005)),  $Z^*$  is given by:

$$Z^* = Z' + jZ'', \quad \text{where } Z' = \frac{R}{1+(\omega\tau)^2} \text{ and } Z'' = -R \left( \frac{\omega\tau}{1+(\omega\tau)^2} \right) \quad (1)$$

and  $M^*$ , by:

$$M^* = j\omega C_o Z^* = M' + jM'', \quad \text{where } M' = \frac{C_o}{C} \left( \frac{(\omega\tau)^2}{1+(\omega\tau)^2} \right) \text{ and } M'' = \frac{C_o}{C} \left( \frac{\omega\tau}{1+(\omega\tau)^2} \right) \quad (2)$$

In these expressions,  $C_o = \frac{\epsilon_0 S}{d}$  is the capacitance of the material in vacuum where  $S$  is the area of the electrode,  $d$  is the thickness of the sample and  $\epsilon_0$  is the permittivity of free space.  $R$  and  $C$  represent the resistance and the capacitance of the material. The relaxation time  $\tau$  satisfies the condition  $2\pi f_o \tau = 1$  where  $f_o$  is the frequency at which the curve  $Z''$  versus frequency presents a minimum. This minimum must correspond to a maximum in  $M''$  versus frequency.

The behaviour of the electrical circuits of Resistance-Capacitance ( $R-C$ ) or Resistance-Constant Phase Element ( $R-CPE$ ) type connected in parallel describes the experimental results in semiconducting materials. The complex impedance, defined for a series of values of the frequency, of the current and voltage, can be represented in different diagrams. The impedance spectrum can be represented in two different modes, Nyquist ( $Z'' = f(Z')$ ) and Bode ( $Z''$  and  $Z' = f$  (frequency)). Bode's representation offers a complete view of the frequency domain, on this representation, the phase shift  $\phi$  as well as the module of the impedance  $|Z^*|$  are plotted as a function of frequency. On the other hand, the most used graphic representation concerns the imaginary part  $Z'' = \text{Im}(Z^*)$  as a function of the real part  $Z' = \text{Re}(Z^*)$  of the complex impedance  $Z^*$ . It is to be understood in three dimensions (frequency  $f$ ,  $Z'$  and  $Z''$ ). These two representations give different visualizations of the same result but they are complementary; each of them shows a particular aspect of the impedance diagram. The Nyquist representation gives detailed information about the studied system, such as relaxation frequency, diameters of semicircles, etc., but sometimes obscures high frequency results while Bode's representation offers a complete view of the domain of frequency, while being less meaningful in identifying certain characteristic phenomena. These two diagrams are illustrated in Fig.2 for a simple  $RC$  circuit.

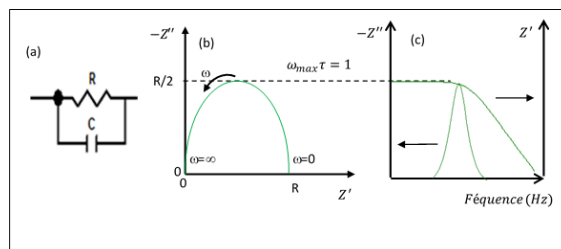


Fig. 2: Simple  $RC$  circuit Model (a), Nyquist (b) and Bode (c) diagrammes.

Figure 3 shows the variation of  $Z''$  versus  $Z'$  for several representative temperatures in the case of rammed earth. An equivalent circuit of  $[(R_{gb} // CPE_{gb}) + (R_g // CPE_g)]$  for the grain ( $R_g$ ,  $CPE_g$ ) and grain boundary ( $R_{gb}$ ,  $CPE_{gb}$ ) contributions is used to fit the experimental data. The impedance of the constant phase element  $CPE_i$  is given by  $Z_{CPE_i} = \frac{1}{Q_i(j\omega)^n_i}$  (Elliot (1987), Jonscher (1983)).

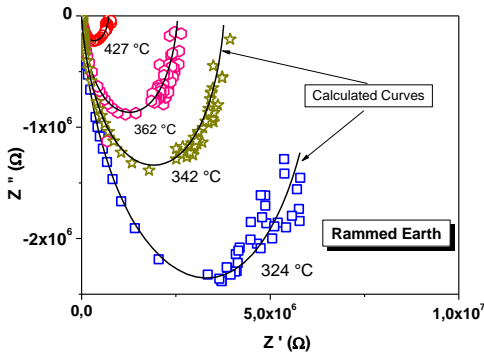


Fig. 3: Experimental and calculated Variation of  $Z''$  as a function of  $Z'$  of Rammed earth for some representative temperatures.

Figure 4 show the variation of the imaginary part ( $Z''$ ) of the complex impedance with frequency for various temperatures for the investigated Kaolin sample. Only one single peak is observed at certain frequency ( $f_0$ ) suggesting the existence of a single contribution in all samples. These peaks shift towards high frequencies when the temperature increases, indicating the relaxation behaviour. In addition, a peak broadening is noticed with increasing temperature, which suggests the presence of a distribution of relaxation times in this material.

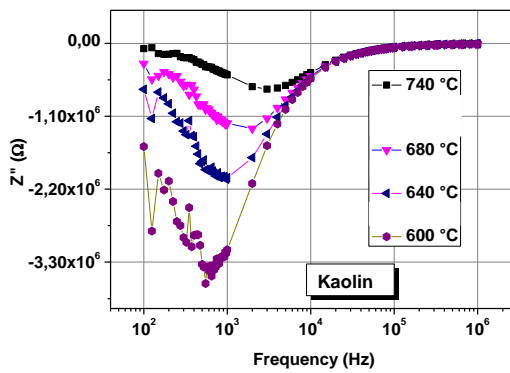


Fig. 4:  $Z''$  as a function of frequency of Kaolin for some representative temperatures.

Figure 5 shows the variation of  $Z''$  versus  $Z'$  for several representative temperatures in the case of Bentonite. Here again as in the case of the rammed earth and kaolin, the observed depressed semicircles indicates the predominance of the grain contribution to the electrical conduction and the distribution of the relaxation time in these clay materials.

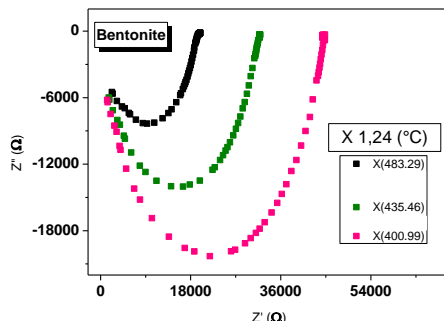


Fig. 5: Experimental and calculated Variation of  $Z''$  as a function of  $Z'$  of Bentonite for some representative temperatures.

#### 4 CONCLUSIONS

Some new experimental data of high temperature impedance spectroscopy are presented in this work for three clay materials: Rammed earth, Kaolin and Bentonite. The data show depressed semicircles indicating the predominance of the grain contribution to the electrical conduction and the distribution of the relaxation time in these systems. More analysis is needed to identify the dominant conduction mechanism of polaron and carriers tunnelling.

## REFERENCES

1. Chandra S., Berntsson L., New York, Editions Andrew Publishing Norwich, 2002.
2. Yongkang Huang, Xinyun Zhai, Tengfei Ma, Mengzhen Zhang, Haobo Pan, William Weijia Lu, Xiaoli Zhao, Tianwei Sun, Yuqiao Li, Jie Shen, Chunhua Yan, Yaping Du, Coordination Chemistry Reviews, 2022, 450, 214236.
3. Saidi M., Cherif A.S., Zeghamati B., Sediki E., Construction and Building Materials, 2018, 167, 566.
4. Medjelekh D., Ulmet L., Dubois F., Energy Procedia, 2017, 139, 487.
5. Miccoli L., Müller U., Fontana P., Construction and Building Materials, 2014, 61, 327.
6. Bouferra R., Marín G., Amhil S., Wasim S.M., Essaleh L., Physica B: Condensed Matter, 2019, 565, 14.
7. Amhil S., Choukri E., Ben Moumen B., Bourial B.
8. Essaleh L., Wasim S.M., Marín G., Rincon C., Amhil S., Galibert J., Journal of Applied Physics, 2017, 122, 015702.
9. Essaleh L., Amhil S., Wasim S.M., Marín G., ChoukriE., Physica E: Low-dimensional Systems and Nanostructures, 2018, 99, 37.
10. Kirou H., Atourkia L., Essaleh L., Taleb A., Messous M.Y., Bouabid K., Nya N., Ihlal A., Journal of Alloys and Compounds, 2019, 783, 524.
11. Bouchehma, L. Essaleh, G. Marín, M. Essaleh, S.M. Wasim, S. Amhil, A. Bourezza, R. Bouferra, S. Belhouideg, Physica B: Condensed Matter, 2021, 622, 413356.
12. El Fgaier F., Lafhaj Z., Chapiseau C., Antczak E., Journal of Building Engineering. 2016, 6, 86.
13. Barsoukov E., Macdonald J.R., Impedance Spectroscopy: Theory, Experiment, and Applications, Wiley, New York, 2005.
14. Elliot S.R., Adv. Phys., 1987, 36, 135.
15. Jonscher A.K., Dielectric Relaxation in Solids, Chelsea Dielectrics Press, London, 1983.